LTV equalization of CPM signals over doubly-selective aeronautical channels

Donatella Darsena
Dipartimento di Ingegneria
Università Parthenope di Napoli, Italy
Email: darsena@uniparthenope.it

Giacinto Gelli, Francesco Verde
Dipartimento di Ingegneria Elettrica e Tecnologie dell'Informazione
Università Federico II di Napoli, Italy
Email: [gelli,f.verde]@unina.it

Ivan Iudice
Communication Systems Laboratory
Italian Aerospace Research Centre
Capua (CE), Italy
Email: i.iudice@cira.it

***Abstract*—In this paper, transmission of continuous phase modulated (CPM) signals over time- and frequency-selective (i.e., doubly-selective) channels is considered. Leveraging on the well-known Laurent representation for a CPM signal, we design a two-stage receiver, composed of a linear time-varying (LTV) equalizer, followed by a detector: the former one aims at mitigating the channel dispersion and it is synthesized under the zero-forcing (ZF) or minimum mean-square error (MMSE) criterion; the latter one recovers the transmitted symbols from the pseudo-symbols of the Laurent representation in a simple recursive manner. Relying on a Basis Expansion Model (BEM) of the doubly-selective channel, we derive frequency-shift (FRESH) versions of the proposed LTV equalizers, discussing also their complexity issues and proposing simplified implementations. Monte Carlo simulation results, carried out in two typical aeronautical scenarios (arrival/takeoff and en-route), show that the proposed approach is able to work satisfactorily also over rapidly time-varying channels.**

***Index Terms*—Continuous phase modulation (CPM), linear time-varying (LTV) equalization, basis expansion model (BEM), frequency-shift (FRESH) filtering, doubly-selective channels, aeronautical telemetry.**

I. Introduction

Continuous phase modulated (CPM) [1] signals are widely employed for telemetry data trasmission in aeronautical applications, due to its many advantages, such as constant envelope properties, spectral efficiency, and noise robustness. Indeed, the IRIG-106 standard [2] adopts different CPM modulation techniques, starting from legacy PCM/FM and SOQPSK, to the most advanced multi-h ARTM one.

Since CPM is a modulation with memory, its main drawback is the high computational complexity of the optimal maximum-likelihood (ML) detection strategy. This issue can be tackled by exploiting the inherent trellis structure of CPM and resorting to the Viterbi algorithm (VA) [3].

D. Darsena, G. Gelli, and F. Verde are also with Consorzio Nazionale Interuniversitario per le Telecomunicazioni (CNIT), Research Unit of Napoli. Their work was partially supported by the Projects "Work Into Shaping Campania's Home (WISCH): Sistemi di trasmissione dati terra-bordo ad elevata capacità" and "TELEMACO: Enabling technologies and innovative electronic scanning systems in millimetre and centimetre bands for avionic radar applications". The work of I. Iudice was partially supported by MIUR through the Project oriented to the development of enabling technologies for RPAS vehicles (TECVOL-II).

In aeronautical communications, due to the high-speed of the aircrafts, the wireless channel might exhibit joint frequency and time selectivity: when CPM is employed over such *doubly-selective* channels, optimal ML detection becomes prohibitive, due to the huge number of states of the VA and the need to perform fast channel estimation and tracking.

Several approaches aimed at reducing the complexity of the ML receiver have been proposed, mostly targeted at time-invariant channels. A popular approach [4], [5], [6] performs preliminary frequency-domain channel equalization to mitigate the effects of intersymbol interference (ISI), allowing thus the subsequent VA to work in an almost ISI-free setting, albeit with colored noise. However, frequency-domain equalization is not a computationally advantageous strategy when the channel is rapidly time-varying, since in this case the channel cannot be diagonalized by a channel-independent transformation of the received data [7], [8], [9].

In this paper, we tackle the problem of receiving a CPM signal over a doubly-selective channel by designing a linear time-varying (LTV) equalizer. The proposed equalizer leverages on the well-known Laurent decomposition [10] of a CPM signal to perform LTV-ZF or LTV-MMSE equalization in the time domain. Moreover, by exploiting the basis expansion model (BEM) [11] for the doubly-selective channel, we derive convenient frequency-shift (FRESH) implementations of the proposed LTV-ZF and LTV-MMSE equalizers, showing that they can be implemented as a parallel bank of linear time-invariant (LTI) filters having, as input signals, different frequency-shifted versions of the received data. The performance of the proposed FRESH receivers is assessed by Monte Carlo computer simulations, showing that they outperform their LTI counterparts over typical aeronautical channels.

A. Notations

Besides standard notations, we adopt the following ones: matrices [vectors] are denoted with upper [lower] case boldface letters (e.g., $\mathbf{A}$ or $\mathbf{a}$); $(\cdot)^*$, $(\cdot)^{\mathrm{T}}$, $(\cdot)^{\mathrm{H}}$, $(\cdot)^{-1}$, $(\cdot)^-$ denote the conjugate, the transpose, the Hermitian (conjugate transpose), the inverse, and the generalized(1)-inverse [12] of a matrix, respectively; $\mathbf{0}_m \in \mathbb{R}^m$, $\mathbf{O}_{m\times n} \in \mathbb{R}^{m\times n}$, and $\mathbf{I}_m \in \mathbb{R}^{m\times m}$ denote the null vector, the null matrix, and the identity matrix,

respectively; $\otimes$ denotes the Kronecker product, $(\cdot)_R$ denotes the modulo-R operation, and $\mathbb{E}[\cdot]$ denotes ensemble averaging

II. System model

Let us consider a wireless communication system employing a binary full-response[1] CPM modulation format with baud-rate $1/T$, whose complex envelope is given [3] by:

$$x_a(t) = \exp\left[j2\pi h \sum_{i=-\infty}^{+\infty} a(i)\, q(t - i\,T) \right] . \qquad (1)$$

In (1), h (assumed to be noninteger) is the modulation index, $a(i) \in \{\pm 1\}$ is the binary symbol sequence, $q(t) \triangleq \int_{-\infty}^{t} f(u)\,\mathrm{d}u$ is the phase response, and $f(t)$ is the frequency response, with $f(t) \equiv 0$ for each $t \notin [0, T]$, $f(t) = f(T - t)$, and $\int_0^T f(t)\mathrm{d}t = q(T) = 1/2$.

For a full-response CPM signal, the Laurent decomposition [10] of $x_a(t)$ reduces to a single PAM component:

$$x_a(t) = \sum_{i=-\infty}^{+\infty} s_0(i)\, c_{a,0}(t - iT) \qquad (2)$$

where the *pseudo-symbol* sequence

$$s_0(i) \triangleq \exp\left[j\pi h \sum_{\ell=-\infty}^{i} a(\ell) \right] \qquad (3)$$

is a nonlinear function of the sequence $a(i)$, while $c_{a,0}(t)$ is a real-valued pulse (see [10] for the detailed expression) whose support is $[0, 2T]$.

The CPM signal given by (1) or (2) is up-converted to radio-frequency (RF) and transmitted over a wireless channel; the received distorted signal, corrupted by AWGN, is filtered and sampled. To obtain a compact discrete model for the overall communication system, we assume that the CPM signal is well represented by its samples $x(k) \triangleq x(kT_\mathrm{c})$ taken with rate $1/T_\mathrm{c} \triangleq N/T$, with $N > 1$ denoting the *oversampling factor*. Denoting with $h_a(t, \tau)$ the overall time-varying channel impulse response (including also the effects of transmit/receive filters), we assume that **(a1)** the channel spans L_h symbol periods in τ, i.e., $h_a(t, \tau) \equiv 0$ for $\tau \notin [0, L_\mathrm{h} T]$.

Hence, assuming perfect synchronization, the complex envelope of the received signal, at the output of the receiver filter, can be expressed as

$$r_a(t) = \sum_{\ell=-\infty}^{+\infty} \sum_{\eta=0}^{N-1} x^{(\eta)}(\ell)\, h_a\left(t, t - \ell T - \eta T_\mathrm{c}\right) + v_a(t) \qquad (4)$$

where $v_a(t)$ represents filtered AWGN, whereas

$$x^{(\eta)}(\ell) \triangleq x(\ell N + \eta) = \sum_{i=-\infty}^{+\infty} s_0(i)\, c_0^{(\eta)}(\ell - i) \qquad (5)$$

due to (2), with $c_0(k) \triangleq c_{a,0}(kT_\mathrm{c})$ and $c_0^{(\eta)}(\ell) \triangleq c_0(\ell N + \eta)$.

[1]For the sake of simplicity, our design assumes a binary single-h full-response CPM signal; the derivations can be extended to partially-response CPM signals as well. Extensions to nonbinary and/or multi-h CPM signals are less tractable and will be the subject of further investigations.

The received signal given by (4) is sampled at time instants $t_{k,n} \triangleq kT + nT_\mathrm{c}$, with $k \in \mathbb{Z}$ and $0 \le n \le N - 1$, thus obtaining $r^{(n)}(k) \triangleq r_a(t_{k,n})$ represented by the following *polyphase decomposition* with respect to N:

$$r^{(n)}(k) = \sum_{\ell=0}^{L_\mathrm{h}} \sum_{\eta=0}^{N-1} h^{(n)}(k, \ell N + n - \eta)\, x^{(\eta)}(k - \ell) + v^{(n)}(k) \qquad (6)$$

where $h^{(n)}(k, \ell) \triangleq h(kN + n, \ell)$, where the discrete-time channel $h(k, \ell) \triangleq h_a(kT_\mathrm{c}, \ell T_\mathrm{c})$, due to **(a1)**, is a causal finite impulse response (FIR) system of order NL_h, i.e., $h(k, \ell) \equiv 0$ for $\ell \notin \{0, 1, \ldots, NL_\mathrm{h}\}$, and $v^{(n)}(k) \triangleq v_a(t_{k,n})$.

The following customary assumptions will be considered in the sequel: **(a2)** the information-bearing symbols $a(i) \in \{\pm 1\}$ are modeled as a sequence of independent and identically distributed (i.i.d.) zero-mean random variables, with $\mathbb{E}[a(i)^2] = 1$; **(a3)** the noise samples $\{v^{(n)}(k)\}_{n=0}^{N-1}$ are modeled as mutually independent zero-mean i.i.d. complex circular random sequences, with variance $\sigma_v^2 \triangleq \mathbb{E}[|v^{(n)}(k)|^2]$, statistically independent of $a(i)$ for each $i \in \mathbb{Z}$. In what follows, we further assume that: **(a4)** the noise variance σ_v^2 is either exactly known at the receiver or it is estimated by using data-aided or non-data aided algorithms [13].

By gathering N consecutive samples (6) into the vector $\mathbf{r}(k) \triangleq [r^{(0)}(k), r^{(1)}(k), \ldots, r^{(N-1)}(k)]^\mathrm{T} \in \mathbb{C}^N$, model (6) can be compactly expressed as

$$\mathbf{r}(k) = \sum_{\ell=0}^{L_\mathrm{h}} \mathbf{H}_\ell(k)\, \mathbf{x}(k - \ell) + \mathbf{v}(k) \qquad (7)$$

where, for $i_1, i_2 \in \{0, 1, \ldots, N - 1\}$, the $(i_1 + 1, i_2 + 1)$th element of the time-varying matrix $\mathbf{H}_\ell(k) \in \mathbb{C}^{N \times N}$ is given by $\{\mathbf{H}_\ell(k)\}_{i_1, i_2} = h^{(i_1)}(k, \ell N + i_1 - i_2)$ and $\mathbf{x}(k) \triangleq [x^{(0)}(k), x^{(1)}(k), \ldots, x^{(N-1)}(k)]^\mathrm{T} \in \mathbb{C}^N$, due to (5) and the support properties of $c_0(t)$, can be compactly expressed as

$$\mathbf{x}(k) = \mathbf{C}_0\, \mathbf{s}_0(k) \qquad (8)$$

where, for $i_1 \in \{0, 1, \ldots, N - 1\}$ and $i_2 \in \{0, 1\}$, the $(i_1 + 1, i_2 + 1)$th element of the matrix $\mathbf{C}_0 \in \mathbb{R}^{N \times 2}$ is given by $\{\mathbf{C}_0\}_{i_1, i_2} = c_0^{(i_1)}(i_2)$, and $\mathbf{s}_0(k) \triangleq [s_0(k), s_0(k - 1)]^\mathrm{T} \in \mathbb{C}^2$.

III. Time-varying detection of CPM signals

The first stage of the proposed receiver performs time-varying channel equalization, allowing one to recover the pseudo-symbols $s_0(n)$; in the second stage, we perform simple recursive inversion of the nonlinear mapping (3) between symbols and pseudo-symbols. Although the overall structure is not optimal, it allows one to equalize rapidly time-varying and dispersive channels with an affordable complexity.

A. First stage: front-end time-varying equalization

Hereinafter, we consider a causal LTV equalizer of order $L_\mathrm{e} > 0$, whose input-output relationship, for any $k \in \mathbb{Z}$, is given by $y(k) = \widetilde{\mathbf{f}}^\mathrm{H}(k)\, \widetilde{\mathbf{r}}(k)$, where $\widetilde{\mathbf{f}}(k) \in \mathbb{C}^{N(L_\mathrm{e}+1)}$ is the weight vector of the equalizer, whereas the input data vector $\widetilde{\mathbf{r}}(k) \triangleq [\mathbf{r}^\mathrm{T}(k), \mathbf{r}^\mathrm{T}(k - 1), \ldots, \mathbf{r}^\mathrm{T}(k - L_\mathrm{e})]^\mathrm{T}$ is expressed as

$$\widetilde{\mathbf{r}}(k) = \widetilde{\mathbf{H}}(k)\, \widetilde{\mathbf{x}}(k) + \widetilde{\mathbf{v}}(k) \qquad (9)$$

where

$$\widetilde{\mathbf{x}}(k) \triangleq [\mathbf{x}^{\mathrm{T}}(k), \mathbf{x}^{\mathrm{T}}(k-1), \ldots, \mathbf{x}^{\mathrm{T}}(k-L_{\mathrm{a}}+1)]^{\mathrm{T}} \in \mathbb{C}^{NL_{\mathrm{a}}}$$
$$\widetilde{\mathbf{v}}(k) \triangleq [\mathbf{v}^{\mathrm{T}}(k), \mathbf{v}^{\mathrm{T}}(k-1), \ldots, \mathbf{v}^{\mathrm{T}}(k-L_{\mathrm{e}})]^{\mathrm{T}} \in \mathbb{C}^{N(L_{\mathrm{e}}+1)}$$

with $L_{\mathrm{a}} \triangleq L_{\mathrm{e}} + L_{\mathrm{h}} + 1$, whereas the expression of the time-varying channel matrix $\widetilde{\mathbf{H}}(k) \in \mathbb{C}^{N(L_{\mathrm{e}}+1)\times NL_{\mathrm{a}}}$ is given in (5) at the top of the following page.[2]

Let $d \in \{0, 1, \ldots, L_{\mathrm{a}}\}$ denote a suitable equalization delay, our aim is to reliably estimate the delayed pseudo-symbol $s_0(k-d)$. By (8) it can be inferred that $\widetilde{\mathbf{x}}(k) = \widetilde{\mathbf{C}}_0 \widetilde{\mathbf{s}}_0(k)$, where $\widetilde{\mathbf{C}}_0 \in \mathbb{R}^{NL_{\mathrm{a}}\times(L_{\mathrm{a}}+1)}$ is a block matrix defined as

$$\widetilde{\mathbf{C}}_0 \triangleq \begin{bmatrix} \mathbf{C}_0 & \mathbf{0}_N & \cdots & \mathbf{0}_N \\ \mathbf{0}_N & \mathbf{C}_0 & \cdots & \mathbf{0}_N \\ \vdots & \ddots & \ddots & \vdots \\ \mathbf{0}_N & \ldots & \mathbf{0}_N & \mathbf{C}_0 \end{bmatrix} \tag{6}$$

and $\widetilde{\mathbf{s}}_0(k) = [s_0(k), s_0(k-1), \ldots, s_0(k-L_{\mathrm{a}})]^{\mathrm{T}} \in \mathbb{C}^{L_{\mathrm{a}}+1}$. By substituting in (9) one has

$$\widetilde{\mathbf{r}}(k) = \widetilde{\mathbf{H}}(k)\, \widetilde{\mathbf{C}}_0\, \widetilde{\mathbf{s}}_0(k) + \widetilde{\mathbf{v}}(k)\,. \tag{7}$$

Two common equalization strategies to recover $s_0(k-d)$ are the LTV-ZF and LTV-MMSE one, which are discussed later.

1) LTV-ZF equalizer: In the absence of noise, perfect or *zero-forcing* (ZF) recovery can be obtained by using a time-varying ZF equalizer [8]. Imposing the ZF condition $y(k) = s_0(k-d)$ leads to the following system of linear equations:

$$\widetilde{\mathbf{f}}^{\mathrm{H}}(k)\, \widetilde{\mathbf{H}}(k)\, \widetilde{\mathbf{C}}_0 = \mathbf{e}_d^{\mathrm{T}} \tag{8}$$

with $\mathbf{e}_d = [\overbrace{0, 0, \ldots, 0}^{d}, d, 0, \ldots, 0]^{\mathrm{T}} \in \mathbb{R}^{L_{\mathrm{a}}+1}$. This system is consistent [12] if and only if $\widetilde{\mathbf{C}}_0^{\mathrm{T}}\widetilde{\mathbf{H}}^{\mathrm{H}}(k)[\widetilde{\mathbf{C}}_0^{\mathrm{T}}\widetilde{\mathbf{H}}^{\mathrm{H}}(k)]^{-}\mathbf{e}_d = \mathbf{e}_d$, for all $k \in \mathbb{Z}$. If the matrix $\widetilde{\mathbf{H}}(k)\,\widetilde{\mathbf{C}}_0 \in \mathbb{C}^{N(L_{\mathrm{e}}+1)\times(L_{\mathrm{a}}+1)}$ is full-column rank, i.e., $\mathrm{rank}[\widetilde{\mathbf{H}}(k)\,\widetilde{\mathbf{C}}_0] = L_{\mathrm{a}}+1$, for all $k \in \mathbb{Z}$, it results that $\widetilde{\mathbf{C}}_0^{\mathrm{T}}\widetilde{\mathbf{H}}^{\mathrm{H}}(k)[\widetilde{\mathbf{C}}_0^{\mathrm{T}}\widetilde{\mathbf{H}}^{\mathrm{H}}(k)]^{-} = \mathbf{I}_{L_{\mathrm{a}}+1}$, for all $k \in \mathbb{Z}$, and, then, the system (8) turns out to be consistent independently of the equalization delay d. In this case, the *minimal norm* solution of (8) is given (see, e.g., [12]) by

$$\widetilde{\mathbf{f}}_{\mathrm{ZF}}(k) = \widetilde{\mathbf{H}}(k)\widetilde{\mathbf{C}}_0[\widetilde{\mathbf{C}}_0^{\mathrm{T}}\widetilde{\mathbf{H}}^{\mathrm{H}}(k)\widetilde{\mathbf{H}}(k)\widetilde{\mathbf{C}}_0]^{-1}\mathbf{e}_d\,. \tag{9}$$

Since the condition $\mathrm{rank}[\widetilde{\mathbf{H}}(k)\widetilde{\mathbf{C}}_0] = L_{\mathrm{a}}+1$, for all $k \in \mathbb{Z}$, assures the consistency of the system (8) and, thus, the existence of LTV-ZF equalizers, it seems natural to investigate the rank properties of $\widetilde{\mathbf{H}}(k)\widetilde{\mathbf{C}}_0$. A necessary condition is that $L_{\mathrm{a}}+1 = L_{\mathrm{h}}+L_{\mathrm{e}}+2 \leq N(L_{\mathrm{e}}+1)$, from which

$$L_{\mathrm{e}} \geq \frac{L_{\mathrm{h}}+2-N}{N-1}\,. \tag{10}$$

Equation (10) shows that oversampling ($N > 1$) is necessary to allow for the existence of a FIR ZF equalizer: indeed for $N = 1$ condition (10) cannot be satisfied with a finite L_{e}.

[2]Note that, due to the time-varying assumption for the channel, matrix $\widetilde{\mathbf{H}}(k)$ loses its typical block Toeplitz structure.

2) LTV-MMSE equalizer: It is well known that, for ill-conditioned channel matrices, ZF equalization can introduce moderate-to-high amount of noise enhancement. To counteract this phenomenon, we resort to the MMSE equalizer, whose expression is obtained by minimizing the output mean-square error objective function $\mathrm{MSE}[\widetilde{\mathbf{f}}(k)] \triangleq \mathbb{E}[|y(k) - s_0(k-d)|^2]$. By standard linear algebra, it can be shown that the optimal $\widetilde{\mathbf{f}}(k)$ satisfies for any $k \in \mathbb{Z}$ the following linear system:

$$\mathbf{R}_{\widetilde{\mathbf{r}}\widetilde{\mathbf{r}}}(k)\widetilde{\mathbf{f}}(k) = \mathbf{r}_{\widetilde{\mathbf{r}}s_0}(k) \tag{11}$$

where $\mathbf{R}_{\widetilde{\mathbf{r}}\widetilde{\mathbf{r}}}(k) \triangleq \mathbb{E}[\widetilde{\mathbf{r}}(k)\widetilde{\mathbf{r}}^{\mathrm{H}}(k)] \in \mathbb{C}^{N(L_{\mathrm{e}}+1)\times N(L_{\mathrm{e}}+1)}$ denotes the statistical time-varying correlation matrix of (9), and $\mathbf{r}_{\widetilde{\mathbf{r}}s_0}(k) \triangleq \mathbb{E}[\widetilde{\mathbf{r}}(k)s_0^*(k-d)] \in \mathbb{C}^{N(L_{\mathrm{e}}+1)}$ is the statistical time-varying cross-correlation vector. The solution of (11) reads as

$$\widetilde{\mathbf{f}}_{\mathrm{mmse}}(k) = \mathbf{R}^{-1}_{\widetilde{\mathbf{r}}\widetilde{\mathbf{r}}}(k)\mathbf{r}_{\widetilde{\mathbf{r}}s_0}(k)\,. \tag{12}$$

By (7) and **(a2)–(a3)**, it can be readily obtained that

$$\mathbf{R}_{\widetilde{\mathbf{r}}\widetilde{\mathbf{r}}}(k) = \widetilde{\mathbf{H}}(k)\widetilde{\mathbf{C}}_0\mathbf{R}_{\widetilde{\mathbf{s}}_0\widetilde{\mathbf{s}}_0}\widetilde{\mathbf{C}}_0^{\mathrm{T}}\widetilde{\mathbf{H}}^{\mathrm{H}}(k) + \sigma_v^2\mathbf{I}_{N(L_{\mathrm{e}}+1)} \tag{13}$$
$$\mathbf{r}_{\widetilde{\mathbf{r}}s_0}(k) = \widetilde{\mathbf{H}}(k)\widetilde{\mathbf{C}}_0\mathbf{r}_{\widetilde{\mathbf{s}}_0 s_0} \tag{14}$$

where the exact expression of the entries of the statistical correlation matrix $\mathbf{R}_{\widetilde{\mathbf{s}}_0\widetilde{\mathbf{s}}_0} \triangleq \mathbb{E}[\widetilde{\mathbf{s}}_0(k)\,\widetilde{\mathbf{s}}_0^{\mathrm{H}}(k)] \in \mathbb{C}^{(L_{\mathrm{a}}+1)\times(L_{\mathrm{a}}+1)}$, as well as those of $\mathbf{r}_{\widetilde{\mathbf{s}}_0 s_0} \triangleq \mathbb{E}[\widetilde{\mathbf{s}}(k)s_0^*(k-d)] \in \mathbb{C}^{L_{\mathrm{a}}+1}$, do not depend on k and can be calculated by using the known correlation properties of the pseudo-symbols [10].

B. Second stage: CPM demodulation

The second stage processes the pseudo-symbol estimates at the output of the first stage to recover the transmitted binary sequence $a(i)$. Although more complicated strategies can be considered, we resort herein to a simple CPM demodulator that exploits the recursive representation (3) of the pseudo-symbols.

Let $y(k)$ be the output of the LTV-ZF or LTV-MMSE equalizer, for high signal-to-noise ratio (SNR) values one has

$$y(k) \approx s_0(k-d) = s_0(k-d-1)\exp\left[j\pi h a(k-d)\right] \tag{15}$$

where (3) has been taken into account. Thus, we obtain an estimate $\hat{a}(k-d)$ of $a(k-d)$ as

$$\hat{a}(k-d) = \frac{1}{\pi h}\arg\{y(k)\,y^*(k-1)\}\,. \tag{16}$$

The value $\hat{a}(k-d)$ is finally compared to a threshold to obtain an hard estimate of the transmitted symbol.

IV. Channel BEM and FRESH representation

The synthesis of the first stage in Section III has been carried out without assuming a particular model for the LTV channel. In this section, we exploit the parsimonious CE-BEM representation [11], [7], [14] of the LTV channel to obtain alternative forms of the receivers in the frequency domain, so called FRESH representations [15].

The starting point is to express the discrete-time channel $h(k,\ell)$ in (6) via the CE-BEM as

$$h(k,\ell) = \sum_{q=-Q_h/2}^{Q_h/2} h_q(\ell)\exp\left(j\frac{2\pi}{P}qk\right) \tag{17}$$

$$\widetilde{\mathbf{H}}(k) \triangleq \begin{bmatrix} \mathbf{H}_0(k) & \mathbf{H}_1(k) & \dots & \mathbf{H}_{L_\mathrm{h}}(k) & \mathbf{O}_{N\times N} & \dots & \mathbf{O}_{N\times N} \\ \mathbf{O}_{N\times N} & \mathbf{H}_0(k-1) & \mathbf{H}_1(k-1) & \dots & \mathbf{H}_{L_\mathrm{h}}(k-1) & \ddots & \mathbf{O}_{N\times N} \\ \vdots & \ddots & \ddots & \ddots & \ddots & \ddots & \vdots \\ \mathbf{O}_{N\times N} & \dots & \ddots & \mathbf{H}_0(k-L_\mathrm{e}) & \mathbf{H}_1(k-L_\mathrm{e}) & \dots & \mathbf{H}_{L_\mathrm{h}}(k-L_\mathrm{e}) \end{bmatrix} \tag{5}$$

with $k \in \mathcal{K}$ and $\ell \in \{0,1,\dots,NL_\mathrm{h}\}$, where the set $\mathcal{K} \triangleq \{k_0N, k_0N+1,\dots,k_0N+N-1,(k_0+1)N,(k_0+1)N+1,\dots,(k_0+K-1)N+N-1\}$ is the observation window of finite length $K>1$ (expressed in symbols), with $k_0 \in \mathbb{Z}$, L_h is the channel length (expressed in symbols), $P \geq KN$, $Q_h \triangleq \lceil 2f_{\max}PT_\mathrm{c}\rceil$, and $f_{\max}$ denotes the Doppler spread of the channel.

When the CE-BEM is *oversampled*, i.e., $P > KN$, model (17) ensures a better level of accuracy in approximating many wireless channels. Hereinafter, we assume that: **(a5)** the coefficients $\{h_q(\ell)\}_{q=-Q_h/2}^{Q_h/2}$ are perfectly known at the receiver, $\forall \ell \in \{0,1,\dots,NL_\mathrm{h}\}$, which can be estimated blindly [11], [16], [17], [18] or by means of training sequences [19], [20].

By employing (17), matrix $\widetilde{\mathbf{H}}(k)$ in (7) can be written as

$$\widetilde{\mathbf{H}}(k) = \sum_{q=-Q_h/2}^{Q_h/2} \widetilde{\mathbf{H}}_q \exp\left(j\frac{2\pi}{P}qkN\right) \tag{18}$$

where $\widetilde{\mathbf{H}}_q \triangleq \mathbf{J}_q\mathbf{H}_q \in \mathbb{C}^{N(L_\mathrm{e}+1)\times NL_\mathrm{a}}$, with $\mathbf{J}_q \triangleq \mathrm{diag}(\mathbf{I}_N, e^{-j\frac{2\pi}{P}qN}\mathbf{I}_N,\dots,e^{-j\frac{2\pi}{P}qL_\mathrm{e}N}\mathbf{I}_N)$, and $\mathbf{H}_q \in \mathbb{C}^{N(L_\mathrm{e}+1)\times NL_\mathrm{a}}$ is an upper-triangular block Toeplitz matrix, whose first N rows are given by $[\mathbf{H}_{0,q},\mathbf{H}_{1,q},\dots,\mathbf{H}_{L_\mathrm{h},q},\mathbf{O}_{N\times N},\dots,\mathbf{O}_{N\times N}]$, where $\{\mathbf{H}_{\ell,q}\}_{i_1,i_2} = h_q(\ell N + i_1 - i_2)\, e^{j\frac{2\pi}{P}qi_1}, \forall i_1,i_2 \in \{0,1,\dots,N-1\}$. If we define $R \triangleq P/N$, then (18) can be equivalently rewritten as

$$\widetilde{\mathbf{H}}(k) = \sum_{p=0}^{R-1} \widetilde{\boldsymbol{\mathcal{H}}}_p \exp\left(j\frac{2\pi}{R}pk\right) \tag{19}$$

where

$$\widetilde{\boldsymbol{\mathcal{H}}}_p \triangleq \begin{cases} \widetilde{\mathbf{H}}_p, & 0 \leq p \leq Q_h/2\,; \\ \mathbf{O}_{N(L_\mathrm{e}+1)\times NL_\mathrm{a}}, & Q_h/2+1 \leq p \leq R-Q_h/2-1\,; \\ \widetilde{\mathbf{H}}_{p-R}, & R-Q_h/2 \leq p \leq R-1\,. \end{cases} \tag{20}$$

It should be noted that (19) is the discrete Fourier series (DFS) expansion, with period R, of the periodically time-varying matrix $\widetilde{\mathbf{H}}(k)$, with $\widetilde{\boldsymbol{\mathcal{H}}}_p$ representing the DFS coefficients. As a consequence, both the LTV-ZF and LTV-MMSE turn out to be also periodic with period R and, thus, they can be expressed by means of their DFS representation over R points:

$$\widetilde{\mathbf{f}}(k) = \sum_{p=0}^{R-1} \widetilde{\mathbf{f}}_p \exp\left(j\frac{2\pi}{R}pk\right) \tag{21}$$

where $\widetilde{\mathbf{f}}_p$ are the DFS coefficients. In the following, we directly obtain expressions for $\widetilde{\mathbf{f}}_p$ for the ZF and MMSE design strategies.

1) FRESH-ZF equalizer: Let $\widetilde{\boldsymbol{\psi}} \triangleq [\widetilde{\mathbf{f}}_0^\mathrm{T},\widetilde{\mathbf{f}}_1^\mathrm{T},\dots,\widetilde{\mathbf{f}}_{R-1}^\mathrm{T}]^\mathrm{T} \in \mathbb{C}^{RN(L_\mathrm{e}+1)}$, by substituting (21) and (19), the ZF condition (8) can be rewritten as

$$\widetilde{\boldsymbol{\mathcal{C}}}_0^\mathrm{T}\widetilde{\boldsymbol{\mathcal{H}}}_{\mathrm{circ}}^\mathrm{H}\widetilde{\boldsymbol{\psi}} = \widetilde{\boldsymbol{\epsilon}}_d \tag{22}$$

where $\widetilde{\boldsymbol{\mathcal{C}}}_0 \triangleq \mathbf{I}_R \otimes \widetilde{\mathbf{C}}_0 \in \mathbb{R}^{RNL_\mathrm{a}\times R(L_\mathrm{a}+1)}$ and the matrix $\widetilde{\boldsymbol{\mathcal{H}}}_{\mathrm{circ}} \in \mathbb{C}^{RN(L_\mathrm{e}+1)\times RNL_\mathrm{a}}$ is block circulant [21] whose $(i+1,j+1)$ block, for $0 \leq i,j \leq R-1$, is given by $\widetilde{\boldsymbol{\mathcal{H}}}_{(i-j)_R} \in \mathbb{C}^{(L_\mathrm{e}+1)\times L_\mathrm{a}}$, i.e.,

$$\widetilde{\boldsymbol{\mathcal{H}}}_{\mathrm{circ}} \triangleq \begin{bmatrix} \widetilde{\boldsymbol{\mathcal{H}}}_0 & \widetilde{\boldsymbol{\mathcal{H}}}_{R-1} & \cdots & \widetilde{\boldsymbol{\mathcal{H}}}_2 & \widetilde{\boldsymbol{\mathcal{H}}}_1 \\ \widetilde{\boldsymbol{\mathcal{H}}}_1 & \widetilde{\boldsymbol{\mathcal{H}}}_0 & \cdots & \widetilde{\boldsymbol{\mathcal{H}}}_3 & \widetilde{\boldsymbol{\mathcal{H}}}_3 \\ \vdots & \vdots & \vdots & \vdots & \vdots \\ \widetilde{\boldsymbol{\mathcal{H}}}_{R-1} & \widetilde{\boldsymbol{\mathcal{H}}}_{R-2} & \cdots & \widetilde{\boldsymbol{\mathcal{H}}}_1 & \widetilde{\boldsymbol{\mathcal{H}}}_0 \end{bmatrix} \tag{23}$$

whereas $\widetilde{\boldsymbol{\epsilon}}_d \triangleq [\mathbf{e}_d^\mathrm{T},\mathbf{0}_{L_\mathrm{a}+1}^\mathrm{T},\dots,\mathbf{0}_{L_\mathrm{a}+1}^\mathrm{T}]^\mathrm{T} \in \mathbb{R}^{R(L_\mathrm{a}+1)}$.

Solution of (22) in the minimal-norm sense is given by

$$\widetilde{\boldsymbol{\psi}}_{\mathrm{ZF}} = \widetilde{\boldsymbol{\mathcal{H}}}_{\mathrm{circ}}\widetilde{\boldsymbol{\mathcal{C}}}_0\left(\widetilde{\boldsymbol{\mathcal{C}}}_0^\mathrm{T}\widetilde{\boldsymbol{\mathcal{H}}}_{\mathrm{circ}}^\mathrm{H}\widetilde{\boldsymbol{\mathcal{H}}}_{\mathrm{circ}}\widetilde{\boldsymbol{\mathcal{C}}}_0\right)^{-1}\widetilde{\boldsymbol{\epsilon}}_d\,. \tag{24}$$

2) FRESH-MMSE equalizer: The starting point for deriving the FRESH version of the MMSE solution is equation (11). By taking into account (13) and (19), it can be proven that $\mathbf{R}_{\widetilde{\mathbf{r}}\widetilde{\mathbf{r}}}(k)$ admits the DFS expansion

$$\mathbf{R}_{\widetilde{\mathbf{r}}\widetilde{\mathbf{r}}}(k) = \sum_{p=0}^{R-1} \boldsymbol{\mathcal{R}}_{\widetilde{\mathbf{r}}\widetilde{\mathbf{r}}}^{[p]} \exp\left(j\frac{2\pi}{R}pk\right) \tag{25}$$

where the DFS coefficients $\{\boldsymbol{\mathcal{R}}_{\widetilde{\mathbf{r}}\widetilde{\mathbf{r}}}^{[p]}\}_{p=0}^{R-1}$ are referred to as the *cyclic correlation matrices* [15] of $\widetilde{\mathbf{r}}(k)$. By substituting (19), (21), and (25), eq. (11) can be expressed as

$$\boldsymbol{\mathcal{R}}_{\mathrm{circ}}\widetilde{\boldsymbol{\psi}} = \widetilde{\boldsymbol{\Xi}}\,\widetilde{\mathbf{C}}_0\,\mathbf{r}_{\widetilde{\mathbf{s}}s_0}^{(d)} \tag{26}$$

where $\widetilde{\boldsymbol{\Xi}} \triangleq [\widetilde{\boldsymbol{\mathcal{H}}}_0^\mathrm{T},\widetilde{\boldsymbol{\mathcal{H}}}_1^\mathrm{T},\dots,\widetilde{\boldsymbol{\mathcal{H}}}_{R-1}^\mathrm{T}]^\mathrm{T} \in \mathbb{C}^{RN(L_\mathrm{e}+1)\times NL_\mathrm{a}}$ and $\boldsymbol{\mathcal{R}}_{\mathrm{circ}} \in \mathbb{C}^{RN(L_\mathrm{e}+1)\times RN(L_\mathrm{e}+1)}$ is a block circulant [21] matrix whose $(i+1,j+1)$ block, for $0 \leq i,j \leq R-1$, is given by $\boldsymbol{\mathcal{R}}_{\widetilde{\mathbf{r}}\widetilde{\mathbf{r}}}^{[(i-j)_R]} \in \mathbb{C}^{N(L_\mathrm{e}+1)\times N(L_\mathrm{e}+1)}$, i.e.,

$$\boldsymbol{\mathcal{R}}_{\mathrm{circ}} \triangleq \begin{bmatrix} \boldsymbol{\mathcal{R}}_{\widetilde{\mathbf{r}}\widetilde{\mathbf{r}}}^{[0]} & \boldsymbol{\mathcal{R}}_{\widetilde{\mathbf{r}}\widetilde{\mathbf{r}}}^{[R-1]} & \cdots & \boldsymbol{\mathcal{R}}_{\widetilde{\mathbf{r}}\widetilde{\mathbf{r}}}^{[2]} & \boldsymbol{\mathcal{R}}_{\widetilde{\mathbf{r}}\widetilde{\mathbf{r}}}^{[1]} \\ \boldsymbol{\mathcal{R}}_{\widetilde{\mathbf{r}}\widetilde{\mathbf{r}}}^{[1]} & \boldsymbol{\mathcal{R}}_{\widetilde{\mathbf{r}}\widetilde{\mathbf{r}}}^{[0]} & \cdots & \boldsymbol{\mathcal{R}}_{\widetilde{\mathbf{r}}\widetilde{\mathbf{r}}}^{[3]} & \boldsymbol{\mathcal{R}}_{\widetilde{\mathbf{r}}\widetilde{\mathbf{r}}}^{[2]} \\ \vdots & \vdots & \vdots & \vdots & \vdots \\ \boldsymbol{\mathcal{R}}_{\widetilde{\mathbf{r}}\widetilde{\mathbf{r}}}^{[R-1]} & \boldsymbol{\mathcal{R}}_{\widetilde{\mathbf{r}}\widetilde{\mathbf{r}}}^{[R-2]} & \cdots & \boldsymbol{\mathcal{R}}_{\widetilde{\mathbf{r}}\widetilde{\mathbf{r}}}^{[1]} & \boldsymbol{\mathcal{R}}_{\widetilde{\mathbf{r}}\widetilde{\mathbf{r}}}^{[0]} \end{bmatrix}. \tag{27}$$

Solution of (26) is given by

$$\widetilde{\boldsymbol{\psi}}_{\mathrm{mmse}} = \boldsymbol{\mathcal{R}}_{\mathrm{circ}}^{-1}\,\widetilde{\boldsymbol{\Xi}}\,\widetilde{\mathbf{C}}\mathbf{r}_{\widetilde{\mathbf{s}}s_0}^{(d)}\,. \tag{28}$$

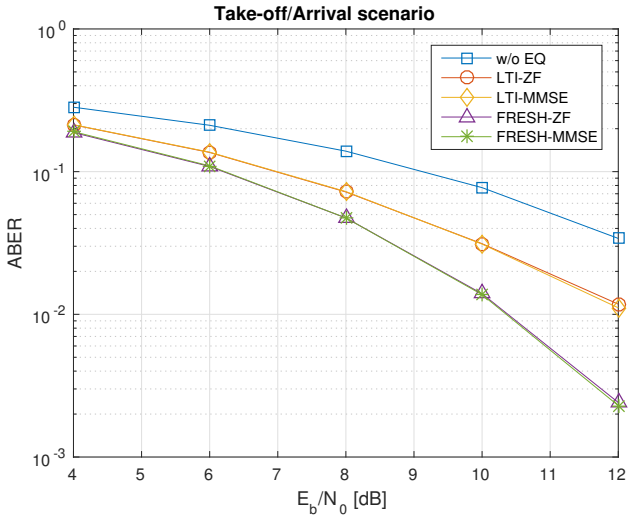

Figure 1. Average BER versus energy contrast for the arrival/takeoff scenario.

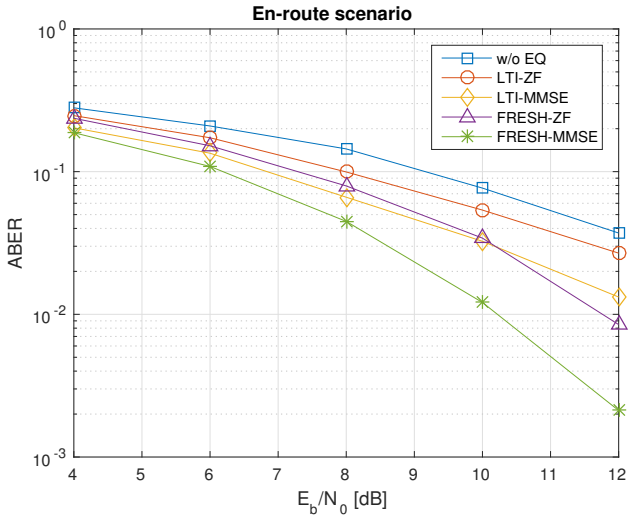

Figure 2. Average BER versus energy contrast for the en-route scenario.

Remark 1: Taking into account (21), the output of the FRESH-ZF or FRESH-MMSE equalizers can be written as $y(k) = \widetilde{\boldsymbol{\psi}}^{\mathrm{H}} \widetilde{\mathbf{z}}(k)$, where $\widetilde{\mathbf{z}}(k) \triangleq \boldsymbol{\zeta}(k) \otimes \widetilde{\mathbf{r}}(k) \in \mathbb{C}^{RN(L_{\mathrm{e}}+1)}$ with $\boldsymbol{\zeta}(k) \triangleq \left[1, e^{-j\frac{2\pi}{R}k}, \ldots, e^{-j\frac{2\pi}{R}(R-1)k}\right]^{\mathrm{T}} \in \mathbb{C}^{R}$. That is, the LTV equalizer can be regarded as a parallel bank of R LTI equalizers, each driven by a different frequency-shifted version of $\widetilde{\mathbf{z}}(k)$.

Remark 2: The FRESH-ZF and FRESH-MMSE solutions require inversion of the large matrices $\widetilde{\boldsymbol{\mathcal{C}}}_0^{\mathrm{T}} \widetilde{\boldsymbol{\mathcal{H}}}_{\mathrm{circ}}^{\mathrm{H}} \widetilde{\boldsymbol{\mathcal{H}}}_{\mathrm{circ}} \widetilde{\boldsymbol{\mathcal{C}}}_0$ or $\boldsymbol{\mathcal{R}}_{\mathrm{circ}}$, respectively [see (24) and (28)]. However, reasoning as in [8], [9], it can be shown that, due to the block circulant nature of such matrices, a much simpler inversion can be carried out operating on the smaller component blocks; moreover, the number of block inverses can be reduced by exploiting the Hermitian symmetry of the overall matrix.

Remark 3: Low-complexity versions of the FRESH-ZF and FRESH-MMSE receivers can be obtained as in [8], [9] by truncating the DFS series of (21) to $Q_e + 1 \ll R$ frequency-shifts. The resulting FRESH implementation consists of a bank of only $Q_e + 1$ LTI equalizers instead of R ones.

V. Numerical results

In this section, we present Monte Carlo computer simulation results aimed at assessing the effectiveness of the proposed LTV-ZF and LTV-MMSE equalizers, implemented in their FRESH versions. We consider a 200 kb/s data link employing a binary full-response CPM modulation format with $h = 2/3$ and rectangular $f(t)$, operating over two typical aeronautical doubly-selective channels: the *Arrival/Takeoff scenario* (AT) and the *En-route scenario* (ER) described in [22], characterized by maximum delay spread values equal to 7 μs and 33 μs, respectively.

The oversampling factor is $N = 4$, the channel length is $L_{\mathrm{h}} = 2$ and $L_{\mathrm{h}} = 7$ for the AT and ER scenarios, respectively, the equalizer length and delay are $L_{\mathrm{e}} = L_{\mathrm{h}} + 1$ and $d = 0$, respectively. Moreover, we considered values of the Doppler spread roughly equal to 1.2 kHz and 3.5 kHz for the AT and ER scenarios, respectively. The parameters of the oversampled BEM model are $K = 100$ and $P = 2KN = 800$, resulting in $R = 2K = 200$, whereas $Q_h + 1 = 5$ and 15 for the AT and ER scenarios, respectively.

As a performance measure, we adopt the average (over 10 channel realizations) bit-error rate (ABER), which is reported as a function of E_b/N_0 in dB.

We compare the performances of the proposed FRESH-ZF and FRESH-MMSE equalizers, implemented assuming perfect knowledge of the channel, with those of their LTI counterparts (LTI-ZF and LTI-MMSE), which are obtained considering a time-averaged version of the same channel. As a reference, we evaluate by simulation also the performances of the receiver that implements only the second-stage, without performing equalization ("w/o EQ" in the plots).

Figure 1 reports the ABER values versus E_b/N_0 ranging from 4 to 12 dB for the AT scenario. First, we observe that, in this scenario, the ZF and MMSE equalization strategies exhibit the same performances, in both the LTV and LTI cases. Moreover, the proposed FRESH equalizers outperform both their LTI counterparts and the "w/o EQ" receiver, especially for moderate-to-high values of E_b/N_0, where the performance gap approaches 2 dB over the LTI equalizers and 3 dB over the "w/o EQ" one.

In Fig. 2, we consider the ER scenario, which is characterized by higher delay and Doppler spread values. Also in this case the proposed FRESH equalizers significantly outperform their LTI counterparts. However, it can be observed that, in this more challenging scenario, the MMSE versions of the LTI and LTV equalizers exhibit better performances than the corresponding ZF versions. In particular, the advantage of using an MMSE approach is apparent in this case, since the FRESH-ZF equalizer performs comparably or even worse than the LTI-MMSE one.

By comparing results of Fig. 1 and Fig. 2, it can be observed that the best receiver (i.e., the FRESH-MMSE equal-

izer) provides almost the same performance in both the AT and ER scenarios. Finally, results not reported here shows that the low-complexity FRESH equalizers implemented by suitably truncating the DFS representation (21) of $\widetilde{\mathbf{f}}(k)$ to $Q_e + 1 \approx 2Q_h \ll R$ coefficients do not show any appreciable performance loss with respect to their ideal versions.

VI. Conclusions

In this paper, LTV equalization strategies for CPM modulated signals operating over doubly-selective channels have been considered. Based on the Laurent representation of a CPM signal, we proposed a two-stage receiver, where the first stage performs LTV-ZF or LTV-MMSE equalization to mitigate the channel selectivity, whereas in the second stage a simple recursive detector recovers the transmitted symbols. By leveraging on the well-known BEM representation for a doubly-selective channel, we derive FRESH implementations of the proposed equalizers. Simulation experiments carried out in two typical aeronautical scenarios confirm the effectiveness of the proposed approach, which is able to equalize the received signal even when the channel is rapidly time-varying.

References

[1] J. Anderson, T. Aulin, and C. Sundberg, *Digital Phase Modulation*. Springer, 2013.

[2] Telemetry Group, Range Commander Council, "Telemetry Standards. IRIG Standard 106-04 Part I," Tech. Rep., May 2004. [Online]. Available: http://www.irig106.org/

[3] J. G. Proakis, *Digital Communications*, 4th ed. McGraw-Hill, 2000.

[4] J. Tan and G. Stuber, "Frequency-domain equalization for continuous phase modulation," *IEEE Transactions on Wireless Communications*, vol. 4, no. 5, pp. 2479–2490, 2005.

[5] F. Pancaldi and G. Vitetta, "Equalization algorithms in the frequency domain for continuous phase modulations," *IEEE Transactions on Communications*, vol. 54, no. 4, pp. 648–658, 2006.

[6] W. Van Thillo, F. Horlin, J. Nsenga, V. Ramon, A. Bourdoux, and R. Lauwereins, "Low-complexity linear frequency domain equalization for continuous phase modulation," *IEEE Transactions on Wireless Communications*, vol. 8, no. 3, pp. 1435–1445, 2009.

[7] I. Barhumi, G. Leus, and M. Moonen, "Time-varying FIR equalization for doubly selective channels," *IEEE Transactions on Wireless Communications*, vol. 4, no. 1, pp. 202–214, 2005.

[8] F. Verde, "Frequency-shift zero-forcing time-varying equalization for doubly selective SIMO channels," *EURASIP Journal on Advances in Signal Processing*, vol. 2006, no. 1, pp. 1–14, 2006.

[9] ——, "Low-complexity time-varying frequency-shift equalization for doubly selective channels," in *Proceedings of the Tenth International Symposium on Wireless Communication Systems (ISWCS 2013)*, 2013, pp. 1–5.

[10] P. Laurent, "Exact and approximate construction of digital phase modulations by superposition of amplitude modulated pulses (AMP)," *IEEE Transactions on Communications*, vol. 34, no. 2, pp. 150–160, 1986.

[11] G. Giannakis and C. Tepedelenlioglu, "Basis expansion models and diversity techniques for blind identification and equalization of time-varying channels," *Proceedings of the IEEE*, vol. 86, no. 10, pp. 1969–1986, 1998.

[12] A. Ben-Israel and T. N. Greville, *Generalized Inverses: Theory and Applications*. Springer, 2003.

[13] M. Boujelben, F. Bellili, S. Affes, and A. Stephenne, "SNR estimation over SIMO channels from linearly modulated signals," *IEEE Transactions on Signal Processing*, vol. 58, no. 12, pp. 6017–6028, 2010.

[14] G. Leus, I. Barhumi, and M. Moonen, "Low-complexity serial equalization of doubly-selective channels," in *Proceedings of Sixth Baiona Workshop on Signal Processing in Communications*, 2003, pp. 69–74.

[15] L. Franks, "Polyperiodic linear filtering," in *Cyclostationarity in Communications and Signal Processing*, W. Gardner, Ed. IEEE Press, 1994, pp. 240–266.

[16] J. K. Tugnait and W. Luo, "Linear prediction error method for blind identification of periodically time-varying channels," *IEEE Transactions on Signal Processing*, vol. 50, no. 12, pp. 3070–3082, 2002.

[17] ——, "Blind identification of time-varying channels using multistep linear predictors," *IEEE Transactions on Signal Processing*, vol. 52, no. 6, pp. 1739–1749, 2004.

[18] F. Verde, "Subspace-based blind multiuser detection for quasi-synchronous MC-CDMA systems," *IEEE Signal Processing Letters*, vol. 11, no. 7, pp. 621–624, 2004.

[19] X. Meng and J. K. Tugnait, "Semi-blind time-varying channel estimation using superimposed training," in *Proceedings of IEEE International Conference on Acoustics, Speech, and Signal Processing (ICASSP '04)*, vol. 3, May 2004, pp. iii–797–800 vol.3.

[20] G. Leus, "On the estimation of rapidly time-varying channels," in *Proceedings of 12th European Signal Processing Conference*, 2004, pp. 2227–2230.

[21] R. A. Horn and C. R. Johnson, *Matrix Analysis*. Cambridge University Press, 2012.

[22] E. Haas, "Aeronautical channel modeling," *IEEE Transactions on Vehicular Technology*, vol. 51, no. 2, pp. 254–264, 2002.